Advances in Science and Technology Research Journal

Advances in Science and Technology Research Journal, 18(8), 96–112
https://doi.org/10.12913/22998624/194144
ISSN 2299-8624, License CC-BY 4.0

Received: 2024.07.10
Accepted: 2024.09.29
Published: 2024.11.01

Analytical, Computer and Laboratory Modelling of the Effect of the Fuel Used in the Spark Ignition Engine of the Selected Vehicle on the Operating Parameters and Exhaust Gas Composition

Karol Tucki[1*], Olga Orynycz[2*], Remigiusz Mruk[1], Ewa Kulesza[2], Paweł Ruchała[3], Grzegorz Wąsowicz[1]

[1] Warsaw University of Life Sciences, Institute of Mechanical Engineering, Department of Production Engineering, Nowoursynowska Street 164, 02-787 Warsaw, Poland

[2] Bialystok University of Technology, Faculty of Engineering Management, Department of Production Management, Wiejska Street 45A, 15-351 Bialystok, Poland

[3] Łukasiewicz Research Network - Institute of Aviation, Aerodynamics Department, Al. Krakowska 110/114, 02-256 Warszawa, Poland

* Corresponding author's e-mail: o.orynycz@pb.edu.pl; karol_tucki@sggw.edu.pl

ABSTRACT

The purpose of the study was to determine the effect of the fuel used in the spark-ignition engine of the selected vehicle on the characteristics of maximum torque and power at the crankshaft of the engine as a function of crankshaft speed and the composition of exhaust gas. The vehicle engine was tested on a stand equipped with V-tech VT-2/B2 chassis dynamometer, MAHA MET 6.3 exhaust gas analyzer and engine parameter monitoring system in compliance with OBD standard. The tests used two commercial fuels with different test octane number (RON) values of 95 and 100 octanes. Measurement of the characteristics of the maximum torque, power on the crankshaft and the total power losses in the drive system, the contact of the wheels with the rollers of the dynamometer and the dynamometer as a function of the crankshaft rotational speed was carried out using the acceleration method with a dynamic load comprising the braking torque of the rotating masses and the electro-swirl brake. On the basis of the test results, engine and drive system parameters of the vehicle, a set of measuring points determining the values of the engine crankshaft speed and the torque generated by the engine crankshaft was determined, using the software for generating driving test runs "the calculation of gearshift points for the WLTC cycle". The parameters of the selected engine operating conditions were within the ranges specified by the software for generating the selected test runs. The content of selected exhaust gas components (carbon monoxide (CO), carbon dioxide (CO_2), other hydrocarbons (HC), oxygen (O_2), λ coefficient, nitrogen oxides (NO) and nitrogen dioxide (NO_2)) was measured for the selected operating parameters of the vehicle for the tested fuels. On the basis of the results of the toxicity measurements, analytical models determining the content of individual components in the exhaust gases as a function of the crankshaft rotational speed and the torque generated on the crankshaft and software simulating the exhaust emissions of the selected vehicle moving under dynamic conditions were developed.

Keywords: engine, fuel, emission, exhaust gases, analysis.

INTRODUCTION

The changing legal environment regarding exhaust emission standards drives rapid development of the fuel and car engine markets [1–3]. There is progress in conventional and alternative fuels. Electric and hydrogen engine technologies in motor vehicles are financially promoted. In order to determine the quality of fuel for internal combustion engines, a various research methods are used in chemical laboratories. The final verification of the fuel should always end on test stand with combustion engines [4–6]. The basic assessment of the quality of fuel used in petrol and diesel engines is carried out in single-cylinder, four-stroke research engines with variable compression ratio, determining the tendency of diesel fuel to self-ignition, expressed by the cetane number and the resistance of petrol to knocking combustion, expressed by octane numbers [7,8].

Octane numbers (tested octane number (TON), motor octane number (MON)) are a measure of the resistance to knocking (detonation) combustion of fuels intended to spark-ignition engines. For motor fuels, octane number is determined by comparing the resistance of the tested fuel to knocking combustion with the resistance of the mixtures of reference fuels with known octane numbers (isooctane and n-heptane) to knocking combustion, under standardised test conditions. An electromechanical detonometer is used for this purpose with a standardised knocking intensity achieved by changing the compression ratio.

The combustion process depends on many factors and on the engine design itself, but it is largely dependent on the chemical composition of the fuel. The higher the compression ratio used, the greater the need for protection against detonation combustion, so the octane number must be correspondingly higher [9–10].

In Europe, two types of petrol are mainly used to power combustion engines. They differ in octane number, having 95 or 98 octanes. Outside the European Union, other procedures for determining the octane number are often used. 98 and 95 petrols differ in composition and additives. 98 petrol is often used in sports models of Japanese vehicle makes, such as: Honda Civic Type R, Toyota GT-86, Subaru Impreza WRX STI or Mitsubishi Lancer Evo. European manufacturers usually decide to adapt their engines to 95 petrol. As part of engine modifications, a compressor or turbocharger is often used to increase the compression ratio, which allows a larger amount of mixture to be forced into the cylinder, which leads to the increased pressure. Modern engines are equipped with a knocking combustion sensor, which checks whether uncontrolled detonations occur in the combustion chamber when powered by 95 octane petrol [11–13].

In 2018, a unified fuel naming system was introduced in the European Union. From January 2024, at Polish petrol stations, petrol with an octane number of 95 (E5) has been replaced with E10 petrol (petrol with a share of biocomponents increased to 10%). However, the so-called Premium petrol with an octane number of 98 will continue to be sold in the E5 format. The additive used in these fuels is second-generation bioethanol (made from agricultural production residues, primarily cereal straw). The change at gas stations is the result of EU regulations requiring Poland to achieve 14% consumption of fuels from renewable raw materials used in transport by 2030 [14].

For many years, studies have been carried out on the amount of pollutants emitted by internal combustion engines as a function of the composition of the fuel mixture [15, 16]. In the case of vehicles, this test shall be carried out on the chassis dynamometer [17, 18]. Conventional and alternative fuels are analyzed. Very often such analyses are carried out in the function of driving tests [19, 20]. On the basis of collected data from the chassis brake, physicochemical parameters of fuels, technical parameters of vehicles, quantitative models using neural networks are built. On the basis of this type of research, emission values are projected for other fuel blends, which often differ in their biocomponent content. The manuscript considered the use of two types of ethanol-based fuels: e95 (this fuel consists of gasoline with 5% ethanol added and intended for Flexible Fuel Vehicles, and standard vehicles equipped with spark ignition engines) and e100 (the fuel thus designated consists mainly of ethanol with a purity of about 4%, the rest is water due to the problem of separating water from ethanol in the process of rectification - azeotropic mixture. Fuels available in Europe marked as e100, e95, e85, e20, e10. The e100 fuel is a commercially available fuel to achieve maximum parameters such as torque on the crankshaft of the engine and power.

The aim of the research was to the influence of fuel composition and octane number on exhaust emissions and performance of the engine put under the analysis.

Operational parameters and chemical composition of exhaust gases were tested on the spark ignition engine of a Fiat Grande Punto Sport 2008. The tests carried out on a chassis dynamometer concerned the comparison of power and torque generated by an engine powered by fuels with an octane number of 95 and 100. Exhaust gas composition tests were carried out using the Maha Met 6.3 exhaust gas analyser. The components of the exhaust gases were tested: carbon monoxide (CO); carbon dioxide (CO_2); hydrocarbons (HC); oxygen (O_2); air excess (λ); nitrogen monoxide (NO).

MATERIALS AND METHOD

A chassis dynamometer was used to measure the power and load of the vehicle in order to assess exhaust emissions. The choice of this type of equipment enabled the use of a dynamic measurement mode and a mode supporting the maintenance of constant engine speed. Advanced software used during the research allowed the authors to obtain precise results, which were used to develop charts and analyse the obtained data. The exhaust gas analyser used in the research enabled a precise assessment of the vehicle's exhaust gas composition, which provided a detailed analysis of every measurement.

The vehicle was placed and secured on a chassis dynamometer in accordance with the manufacturer's guidelines. This action ensured stable and safe conditions for carrying out the tests, minimising the risk of damage and ensuring reliable measurement results. The vehicle's fuel was changed from 95 octanes to 100 octanes while the fuel tank was empty. 10 litres of new fuel were poured into the tank and a considerable distance was then driven so that the vehicle operated on 100-octane fuel during the test. First, the maximum engine power was measured, and then exhaust emissions were checked in the constant speed mode.

The vehicle, on which the tests were carried out, was Fiat Grande Punto Sport manufactured in 2008. The vehicle was equipped with a 16-valve 1.4 T-Jet engine with a factory power of 88 kW (120 HP) and torque of 200 Nm (Table 1).

The vehicle had undergone minor modifications. In the intake system, the factory air filter was replaced with a filter insert with lower flow resistance. In addition, a larger diameter downpipe was installed behind the turbocharger, and the catalytic converter was replaced with a high-flow one. For this reason, the actual values measured using a chassis dynamometer would be higher than in case of fully factory vehicles. The aim of these modifications was to increase the maximum engine parameters (power and torque) in relation to the factory values. These are basic modifications carried out by persons or companies that do not require interference with the design of the intake system, exhaust system and ECU control software. The target was achieved because the maximum power of the vehicle according to tests carried out on the chassis brake was 104kW (with a factory value of 88kW). This car has a permanent modification and is in use.

Table 1. Basic technical parameters of the tested vehicle according to the manufacturer

Parameter	Description
Year of Manufacture	2008
Capacity	1368 cm³
Fuel type	95-octane unleaded petrol
Maximum power	88 kW (120 HP) at 5000 rpm
Maximum torque	200 Nm at 1750 rpm
Site of the engine	Front, transverse
Supercharging system	Turbocharged
Camshaft type	DOHC
Number of cylinders	4
Number of valves	16
Compression ratio	10.0:1
Cylinder diameter	72 mm
Piston stroke	84 mm
Injection type	Multi-point (MPI)
Exhaust emission standard	EURO 4
Drive type	Front axle

The tested vehicle was equipped with a manual gearbox with five forward gears and one reverse gear (Table 2).

Equipment used in the research:

- emission probe,
- Emission Software,
- Maha Met 6.3 exhaust gas analyser,
- OBD II (on board diagnostic),
- Chassis dynamometer V-tech, model VT-2/B2.

A V-tech chassis dynamometer, model VT-2/B2, was used to perform power measurements and to load the engine during exhaust gas measurements (Table 3). It is a single-axis dynamometer with two additional eddy current brakes. The VTech Dyno 6 software was used to operate the dyno during measurements.

The computer software, which was included in the basic exhaust gas analyser kit, was connected to the analyser via a Wi-Fi network. The measurement probe was connected to the analyser and OBD II was inserted into a special connector inside the vehicle. Table 4 shows the technical parameters of the Maha Met 6.3 exhaust gas analyser.

The tested vehicle was placed with its front axle on the rollers of a chassis dynamometer (Fig. 1, Fig. 2). The vehicle was pressed to the rollers using special belts passed through the control arm on the front axle. The rear wheels were secured with transport belts and attached to the dynamometer. A mobile turbine fan placed approximately 1 metre

Table 2. Specifications of the gearbox installed in the tested vehicle

Parameter	Description
Gearbox name	Fiat C510.5
Gears 1, 2, 3, 4, 5	With tapered teeth
Reverse gears	With straight teeth
Synchronisers	Conical by Borg-Wagner
Clutch shaft bearing on the clutch side	Ball
Clutch shaft bearing on the rear side	Double row ball
Main shaft bearing on the clutch side	Roller
Main shaft bearing on the rear side	Ball
1st gear ratio	3.909
2nd gear ratio	2.238
3rd gear ratio	1.444
4th gear ratio	1.029
5th gear ratio	0.767
Reverse gear ratio	3.909
Gear of the final drive	Roller with tapered teeth
Final drive ratio	3.563
Total gear ratio of the drive unit in 1st gear	13.928
Total gear ratio of the drive unit in 2nd gear	7.974
Total gear ratio of the drive unit in 3rd gear	5.145
Total gear ratio of the drive unit in 4th gear	3.666
Total gear ratio of the drive unit in 5th gear	2.733
Total gear ratio of the drive unit in reverse gear	13.928
Differential inner housing bearings	Conical

Table 3. Specifications of the dynamometer used to carry out the tests [20]

Specifications	Description
Type	Load
Dimensions (length/width)	1150 mm/3170 mm
Max/min wheelbase	2200 mm/900 mm
Minimum tyre diameter	400 mm
Maximum load on the axle	3000 kg
Number of axles	1
Brakes	2x1000 Nm eddy current brake
Maximum speed	300 km/h
Maximum power in inertia mode	450 kW
Maximum power in dynamic mode and road tests	1000 kW
Maximum power in constant speed mode (wheel power)	540 kW
Power measurement accuracy, inertial mode	0.1%
Power measurement accuracy, braked mode	1%
Power supply (without cooling and exhaust fans)	min. AC 400 V/32 A
Compressed air required	Minimum 6 bar
Default location	Universal

in front of the vehicle's bumper and positioned in a way, which enables proper engine cooling. To ensure the measurement accuracy, the procedure was repeated three times. The purpose of repeating the measurements was to eliminate possible errors. To build the neural model, the "Multilayer Feed Forward Backpropagation Network" neural network structures with approximating properties were used. In the structure of the neural network, non-linear activating functions $f_1(x)$ and $f_2(x)$ defined by the relationship were used in the hidden layers, and in the output layer, a linear activating function $f_3(x)$ was used in the form:

$$f_1(x) = \frac{2}{1 + \exp(-2\sum_{i=1}^{n} w_i x_i + b_i)} \tag{1}$$

$$f_2(x) = \frac{2}{1 + \exp(-2\sum_{i=1}^{n} u_i x_i + b_i)} \tag{2}$$

$$f_3(x) = \sum_{i=1}^{n} v_i x_i + b_i \tag{3}$$

where: b_i – polarity values of neurons in individual layers; x_i – input signals for the neuron; w_i, u_i, v_i – weight values of neurons in individual layers.

Table 4. Values measured by MAHA MET 6.3 [21]

Value	Unit	Measurement range	Measurement accuracy
CO	[%]	0–15	0.01
CO_2	[%]	0–20	0.01
HC	[ppm]	0–30000	1
O_2	[%]	0–25	0.01
λ	–	0–9.99	0.01
PM 10	[mg/m³]	1–1100	1

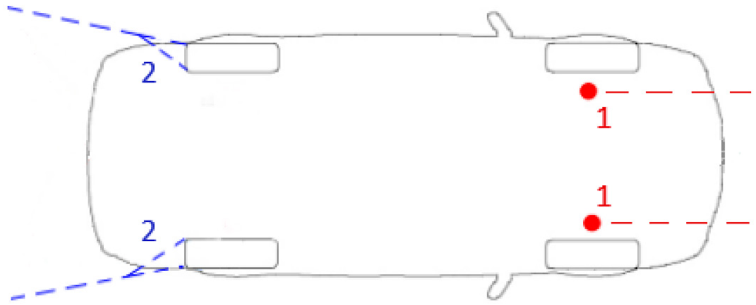

Figure 1. Simplified diagram of the vehicle attached to the dynamometer: 1 – fixing to the control arms, 2 – fixing to the rear wheels

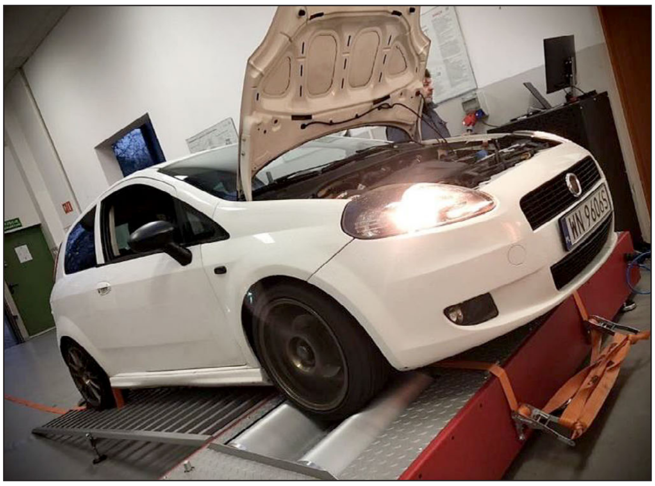

Figure 2. Tested vehicle undergoing tests on a chassis dynamometer

The Levenberg-Marquardt algorithm was used in the network training process, which is based on the optimisation process through finding the minimum value of the objective function defined as the average value of the sum of the squares of the differences between the current values of the network output signals and the values set in the form:

$$\Delta\bar{e}^2 = \frac{1}{m}\sum_{i=1}^{m}(d_i - y_i)^2 \tag{4}$$

where: y_i – learning values set; d_i – values of network responses in the learning process.

Research results

The tests were carried out on 2008 Fiat Grande Punto Sport vehicle equipped with a spark-ignition engine. The research results are presented in charts and tables. The tests were carried out at various engine speeds, and emissions were examined using an exhaust gas analyser.

Determination of engine characteristics

The engine characteristics were determined using a chassis dynamometer. Precision of the equipment ensured accurate readings of the engine power and torque depending on the measurement time and engine crankshaft revolutions (Fig. 3, Fig. 4).

Below there are charts drawn up based on data obtained during maximum power measurements on a chassis dynamometer. The study consisted of three measurements. During each measurement, the engine operated on 95 and 100 octane fuel.

Analyzing Figures 3 and 4, it can be seen that in Figure 3b there is an overlap of the curves from the acceleration test on the chassis dynamometer (test number 1 and 3). This is due to the correctly performed test and repeatability.

Analysing the comparison charts for both types of fuels, significant differences in the performance of the engine in different revolution ranges can be seen. Particularly visible changes can be observed in the mid-speed range, where

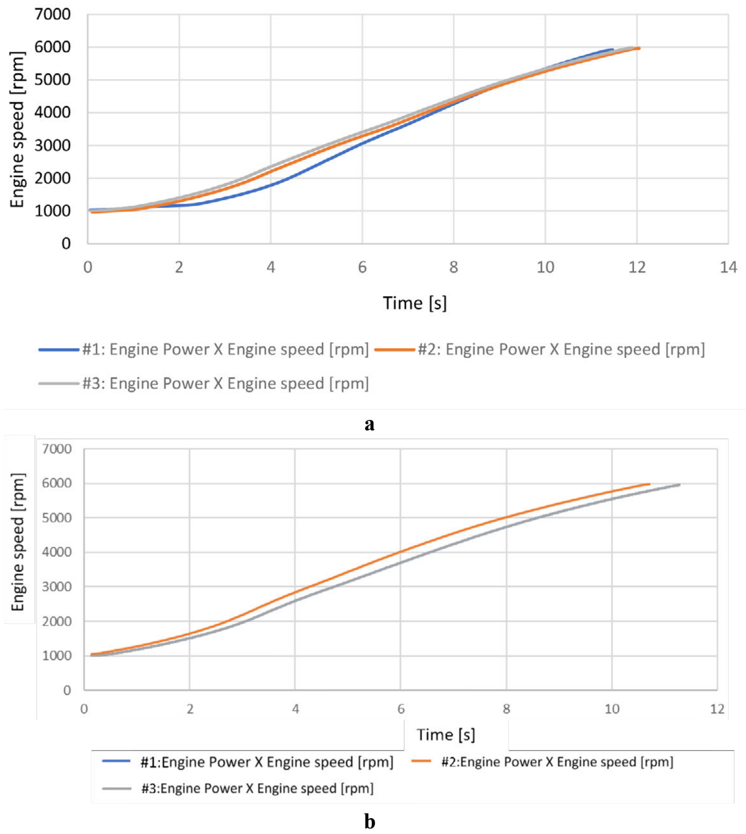

Figure 3. Chart of the engine speed measured during the acceleration test: a – 95 octane fuel, b – 100 octane fuel

Figure 4. Combined chart of engine power and engine crankshaft torque: a – 95 octane fuel, b – 100 octane fuel

a significant increase in torque between 2,200 and 3,800 rpm is noticeable (for e100 rotational speed 2500rpm torque 267Nm, for e95 rotational speed 2500rpm 222Nm, e100 rotational speed 3800 245Nm, for e95 rotational speed 3800 torque 214Nm). Of course, these performance differences are not limited to this rpm range, but are present throughout the entire engine operating spectrum. Despite this noticeable difference in torque, it is worth noting that the engine's maximum power remains almost unchanged. Nevertheless, due to the specificity of the torque increase, especially in the practical range, we see an improvement in the vehicle flexibility. This is important because it translates into better vehicle performance and overall usability in various road conditions. The flexibility of the vehicle is defined as the amount of maximum torque to torque at maximum power. In this case, an increase in maximum torque was observed with the unchanged torque value for maximum power.

Exhaust gas composition testing

Based on the conducted research, a comparison was made of the emission of an engine operating on 95 octane and 100 octane fuels. The results of the exhaust composition tests for two different fuels at engine crankshaft speed and engine torque are shown in Table 5.

The following procedure was used to obtain the measurement results shown in Table 5: using

Table 5. Summary of the results of the exhaust composition test for two different fuels, the change in engine crankshaft speed and engine torque

Octane value [-]	Rotation speed [r/min]	Power [kW]	Torque [Nm]	CO [%]	CO_2 [%]	HC [ppm]	O_2 [%]	λ [-]	NO [ppm]	NO_2 [ppm]
95	1500	3	19.09859	0.52	14.2	216.9	0.835	1.0151	1679.6	0
95	1500	7.2	45.83662	0.52	14.3	208.6	0.665	1.007	2733.8	0
95	1500	11.4	72.57465	0.515	14.3	186.3	0.613	1.0059	3381.9	0
95	1500	15.5	98.67606	0.5	14.31	157.3	0.594	1.0063	3302.8	0
95	2000	4.3	20.53099	0.535	14.3	189	0.692	1.0088	1989.8	0
95	2000	12.9	61.59296	0.524	14.36	180.4	0.541	1.0019	3445.7	0
95	2000	21.5	102.6549	0.52	14.4	141.6	0.502	1.0021	3467.9	0
95	2000	30.1	143.7169	0.523	14.4	104.1	0.448	1.0009	3226.4	0
95	2500	5.7	21.7724	0.616	14.2	191.7	0.756	1.0092	2440.2	0
95	2500	17.7	67.60902	0.57	14.3	170.2	0.569	1.0029	3634	2
95	2500	32.7	124.9048	0.56	14.4	117.9	0.49	1.001	3369.9	0
95	2500	40.7	155.4625	0.54	14.44	88.2	0.417	0.9997	3204.6	0
95	3000	7.2	22.91831	0.591	14.3	144.7	0.692	1.009	2550.6	0
95	3000	21.2	67.4817	0.553	14.39	139.6	0.534	1.0032	3621.1	29.7
95	3000	34.2	108.862	0.794	14.2	108.6	0.584	0.999	3484.9	30.7
95	3000	48.2	153.4254	0.59	14.4	103.3	0.529	1.003	3540.7	26.4
100	1500	3	19.09859	0.506	14.4	187.9	0.823	1.0158	2085.7	0
100	1500	7.2	45.83662	0.515	14.4	168.3	0.682	1.0095	3139.3	36.2
100	1500	11.4	72.57465	0.493	14.5	160	0.642	1.0088	3518.3	42.6
100	1500	15.5	98.67606	0.505	14.49	144.8	0.624	1.008	3175.143	41
100	2000	4.3	20.53099	0.52	14.4	175.6	0.704	1.01	2443.1	0
100	2000	12.9	61.59296	0.53	14.44	164.4	0.579	1.0046	3693	36.9
100	2000	21.5	102.6549	0.509	14.5	127.9	0.547	1.005	3741.4	35.1
100	2000	30.1	143.7169	0.53	14.5	92.2	0.482	1.003	3426.2	23.8
100	2500	5.7	21.7724	0.57	14.37	169.8	0.714	1.0095	2704.4	8.7
100	2500	17.7	67.60902	0.585	14.4	155.3	0.6	1.0042	3944.7	39.6
100	2500	32.7	124.9048	0.559	14.5	96.5	0.492	1.0022	3706.5	25.9
100	2500	40.7	155.4625	0.56	14.5	84.8	0.438	1	3664	0
100	3000	7.2	22.91831	0.61	14.3	154.7	0.718	1.0171	2873.8	2
100	3000	21.2	67.4817	0.577	14.4	141.2	0.57	1.0037	4159.2	36
100	3000	34.2	108.862	0.551	14.5	108.9	0.49	1.002	4114.2	28.2
100	3000	48.2	153.4254	0.67	14.4	96.8	0.558	1.00182	4046.3	32.4

a chassis dynamometer, the correct point of vehicle operating parameters was set, taking into account engine speed and engine load. The loaded vehicle was operated for at least 3 minutes to stabilize the operating conditions. After that, at least ten measurement tests were carried out for the individual quantities considered. The results in the table represent the average values from these measurement trials.

Examination of exhaust gas composition using neural networks

As part of the research work, quantitative models of the content of the substances under consideration in the exhaust gases were prepared.

Table 6 shows the results of fitting quantitative models obtained from the neural network learning process. (ANN – network computing structure; OCT – octane value of fuel [-]; n – crankshaft speed [rpm]; P – engine load index [%]).

In the case of the construction of neural models for the content of O_2, NO, very good parameters of the degree of adaptation of structures to the measurement data were obtained (R^2 above 0.97). On the other hand, the models for CO, HC and λ were characterized by a good degree of fit in the range 0.94 to 0.95. The model based on the neural network for CO_2 did not obtain satisfactory values of the degree of fit to the measurement data (R^2 0.83), which may indicate an increased scattering of the measurement data.

Then, using neural networks, the content of individual substances in the exhaust gases was analysed for the selected vehicle (Fig. 5, Fig. 6, Fig. 7, Fig. 8, Fig. 9, Fig. 10, Fig. 11).

The surfaces of the obtained models shown in Figure 5a and b indicate that the CO content within the range of the engine operating conditions under consideration with the change in rotational speed and torque are characterized by high stability. Figure 5c, on the other hand, shows that for speeds below 2500 rpm, regardless of the torque value, the e95-fuelled engine emitted higher CO values. At higher engine crankshaft speeds, a slight reduction in CO content compared to the e100 fuel-powered engine was observed.

Figures 6a and 6b above show a very stable CO_2 content in exhausts as a function of changes in crankshaft speed and torque load. This reflects the correct operation of the test engine for the composition of the fuel mixture similar to stoichiometric conditions (λ =1). Figure 6c shows the differences between the CO_2 content for an e95 fuel-powered engine and an e100 fuel-powered engine. The e100 fuel-powered engine had a higher CO_2 content overall than the e95 fuel-powered engine.

In the case of Figures 7a and b, the obtained models indicate a slight decrease in HC content as the engine crankshaft speed increases. On the other hand, the increased load leads to a significant reduction in the HC content in the exhaust. Comparing the changes in HC content (for e95, e100 fuel) in the engine load area under consideration on the basis of Figure 7c, it can be seen that the engine powered by e95 fuel obtained higher HC content values compared to the engine powered by e100 fuel.

Graphs 8a and b show the O_2 content curves as a function of speed changes and torque changes for the fuels under consideration. As in the case of CO_2, the graph surfaces indicate very stable values, which result from the specifics of the operation of the spark ignition engine. In the case of Figure 8c, it was noted that for a rotational speed below 2000 rpm the engine obtains fuelled e95 obtains lower oxygen content in the exhausts relative to the e100 fuel. In the mid-range of engine speed (2500rpm) for minimum or maximum torque values, the e95-fuelled engine produces exhausts containing more oxygen than the e100-fuelled engine.

Table 6. Summary of results of matching quantitative models obtained on the basis of the learning process of neural networks

Quantitative model	Number of neurons in the hidden layer [-]	Matching Factor R^2 [-]
CO = ANN(OCT, n, P) [%]	3	0.941909
CO_2 = ANN(OCT, n, P) [%]	1	0.834807
HC = ANN(OCT, n, P) [ppm]	2	0.954155
O_2 = ANN(OCT, n, P) [%]	4	0.975806
λ = ANN(OCT, n, P) [-]	4	0.956957
NO = ANN(OCT, n, P) [ppm]	2	0.976101

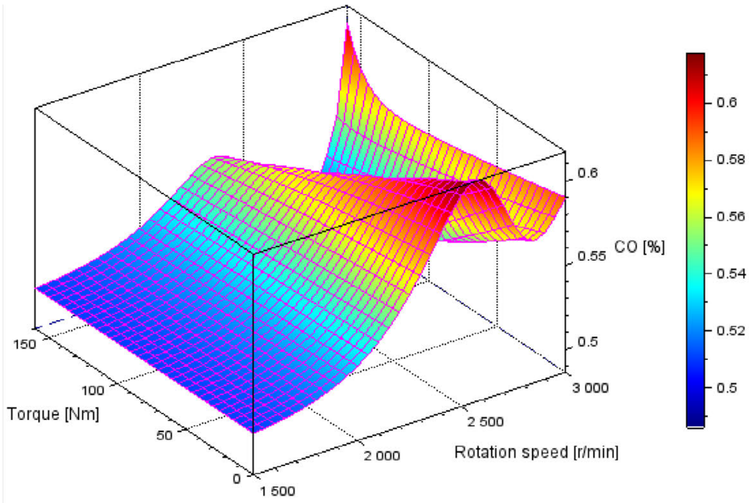

a

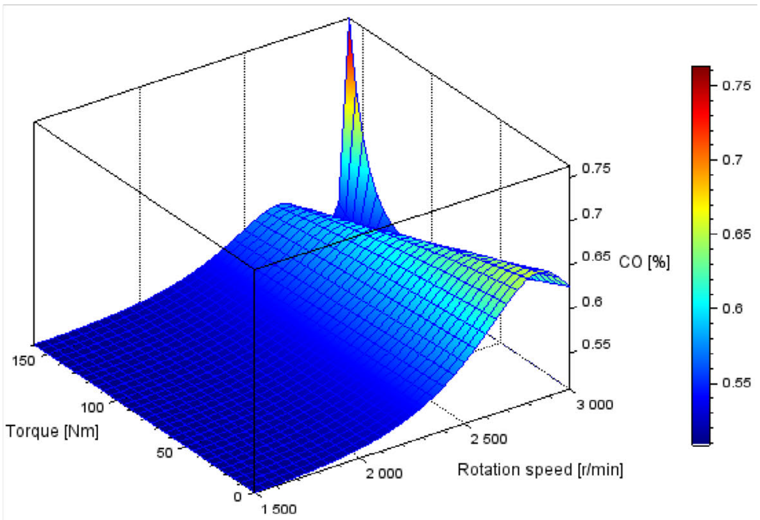

b

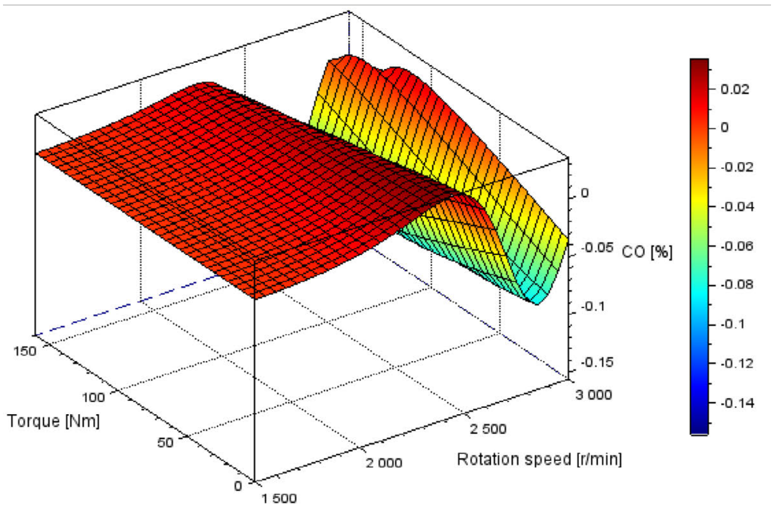

c

Figure 5. Quantitative model of CO [%] changes in exhaust gases as a function of crankshaft speed [rpm] and engine load ratio [%]: a- fuel 95 octanes, b- fuel 100 octanes, c - differences in the course of the obtained quantitative model of CO [%] changes in exhaust gases (values for fuel 95 octanes – values for fuel 100 octanes) as a function of shaft speed [rpm] and the engine load rate [%]

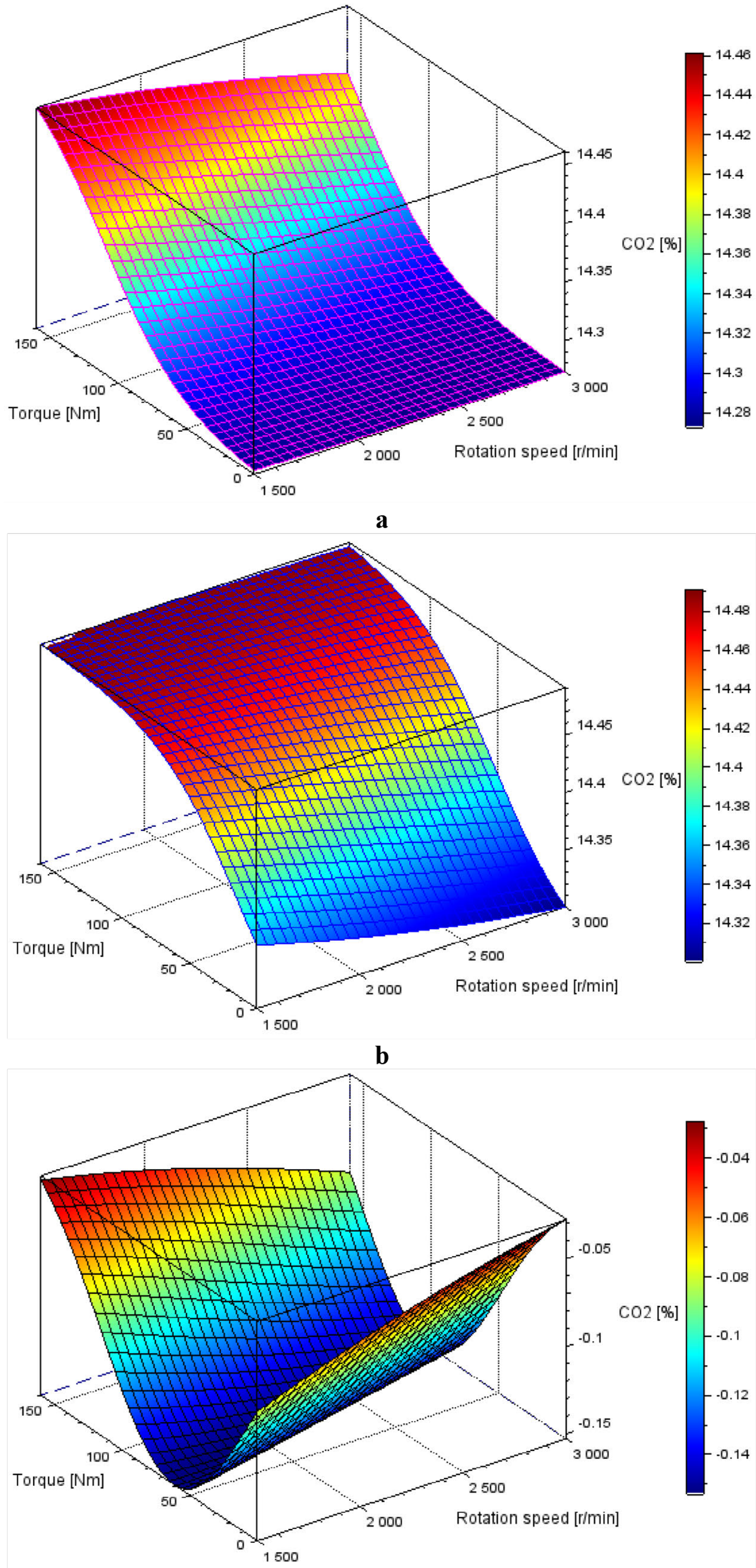

c

Figure 6. Quantitative model of CO_2 change [%] in the exhaust gas as a function of crankshaft speed [rpm] and engine load ratio [%]: a- fuel 95 octanes, b- fuel 100 octanes, c - differences in the course of the obtained quantitative model of CO_2 change [%] in the exhaust gas (values for fuel 95 octanes – values for fuel 100 octanes) as a function of speed crank speed [rpm] and engine load ratio [%]

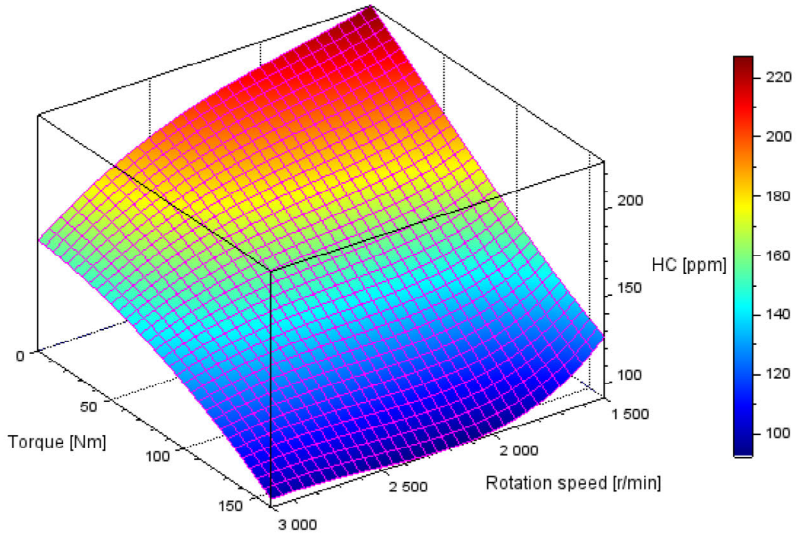

a

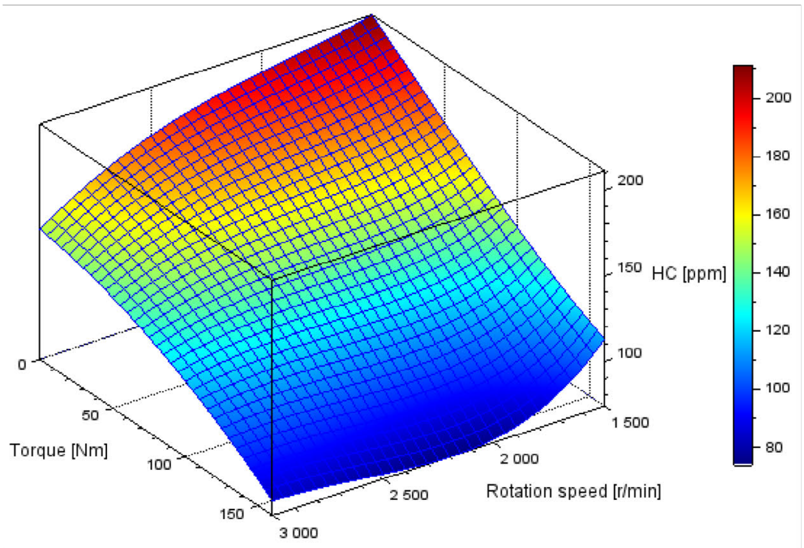

b

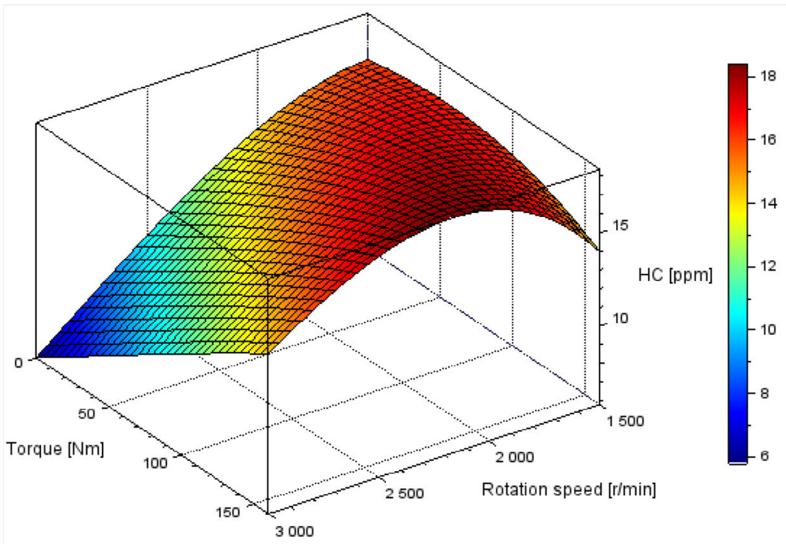

c

Figure 7. Quantitative model of changes in HC content [ppm] in exhaust gas as a function of crankshaft speed [rpm] and engine load ratio [%]: a- fuel 95 octanes, b- fuel 100 octanes, c - differences in the course of the obtained quantitative model of changes in HC content [ppm] in exhaust gas (values for fuel 95 octanes – values for fuel 100 octanes) as a function of shaft speed [rpm] and the engine load rate [%]

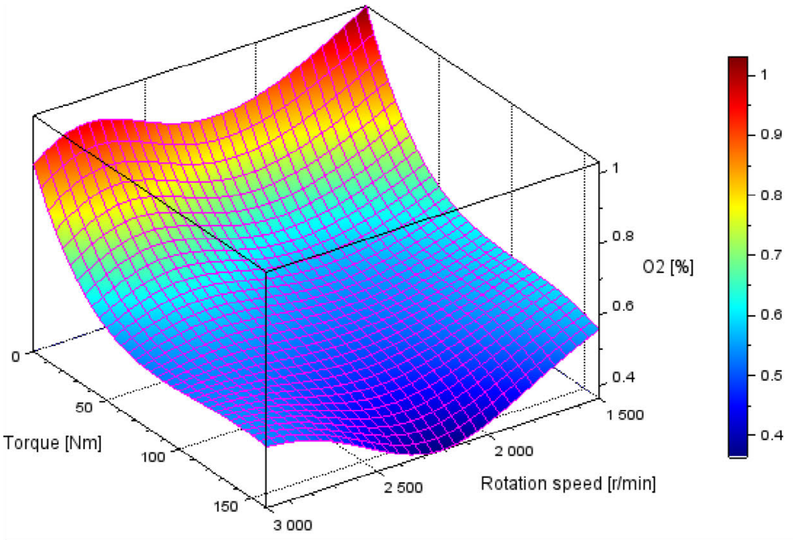

a

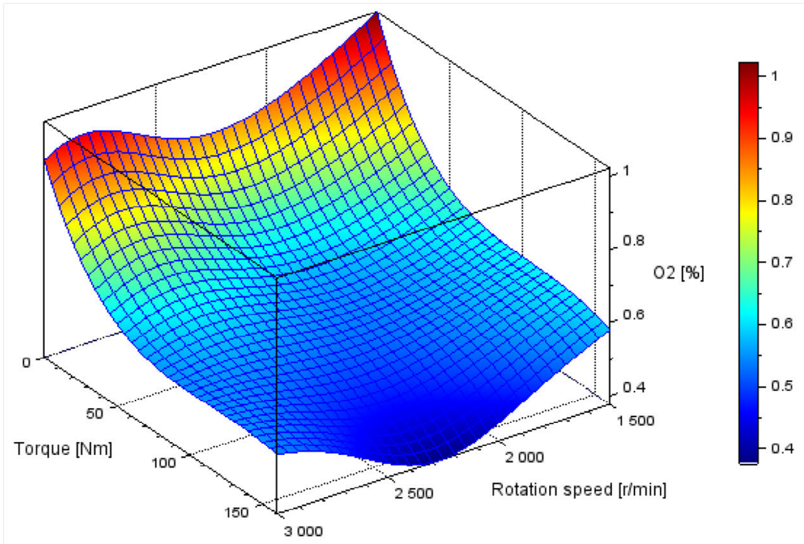

b

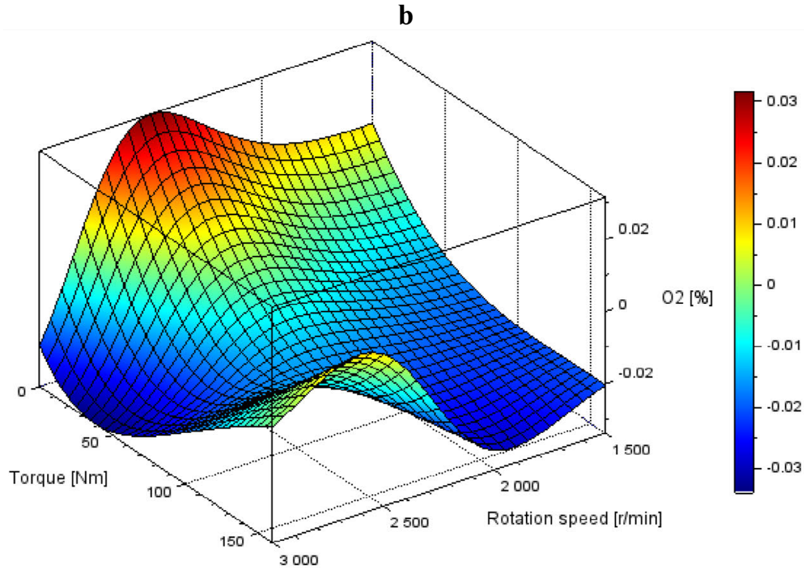

c

Figure 8. Quantitative model of changes of O_2 content [%] in exhaust gases as a function of crankshaft speed [rpm] and engine load ratio [%]: a- fuel 95 octanes, b- fuel 100 octanes, c - differences in the course of the obtained quantitative model of changes of O_2 content [%] in exhaust gases (values for fuel 95 octanes – values for fuel 100 octanes) as a function of crankshaft speed [rev]. min] and the engine load ratio [%]

Figures 9a and 9c show the changes in the λ content of the exhaust factor obtained for tests using e95 and e100 fuels. Built models using neural networks indicate for this parameter a very high stability of the value with changes in the rotational speed and torque of the engine. The obtained runs confirm the correct operation of the tested engine with spark ignition. The differences in these values may be due to the limitations of the engine control systems. Figure 9c shows that the e95 fuel-powered engine obtained lower λ factor values than the e100 fuel-powered engine.

The test engine was characterized for minimum loads by higher values of the Air to fuel ratio (higher values AFR - air to fuel ratio) than for heavy loads (for small loads λ 1.018–1.022, for large loads λ 0.995–1.00).

The obtained models of NO content in exhausts indicate that the engine was characterized by small changes in this parameter in the function of speed and torque for the range above 50 Nm. On the other hand, for a load value below 50 Nm, the reduction in the content of this parameter strongly affects the reduction in the NO content in the exhaust. In the case of Figure 10c, the content comparison for the e95 and e100 powered engine indicates that the e95 fuel-powered engine obtained a higher NO content in the exhaust throughout the range of engine operating conditions (change in speed, torque).

DISCUSSION

To sum up, the test results indicated that 100 octane fuel may be more beneficial in terms of engine performance, but was associated with higher nitrogen oxide emissions and the potential presence of particulate matter. On the other hand, 95 octane fuel was less efficient in terms of power and torque, but lead to lower NO_x emissions. Both performance requirements and environmental issues must be considered when selecting fuel for an engine. 100 octane fuel may be preferred if engine performance is a deciding factor. In turn, 95 octane fuel may be more suitable in situations where the priority is to reduce exhaust emissions, including nitrogen oxides. There is a belief that a higher number of octanes adds power to the engine. That's not true. Petrol with a high octane number will allow you to obtain more power, as it allows you to increase the pressure in the cylinder. However, to achieve this, it is necessary to modify the drive unit, for example by recharging or reducing the combustion chamber.

The introduction of ethanol into the motor gasoline formula affects the physicochemical and functional properties of such fuels [23]. Bioethanol, as an alternative fuel, is interesting because it can be used without major modifications in conventional combustion engines using fossil fuels. However, further research is needed because gasoline and ethanol have different spraying and combustion properties due to differences in their physical properties.

The results of the studies presented in this manuscript confirm the positive impact of combustion of biofuels e95 and e100 on engine power and efficiency. Studies on the impact of E85 biofuel combustion on engine power and efficiency are presented in [24]. In addition to the chemical properties of E85 biofuel and BA95 model fuel, in particular the net fuel value, the efficiency of the internal combustion engine is also influenced by fuel consumption and engine power. In turn, studies in [25] show that as the share of ethanol in the gasoline mixture increases, so does the share of heat released from the combustion of injected fuel. More heat can be converted into mechanical work. Blends containing ethanol burn faster than gasoline without ethanol. All these properties have a direct impact on the engine output parameters and overall engine efficiency. Modelling and prediction of cavitation erosion in e100 fuel-powered GDi injectors was published [26]. The use of e100 fuel poses a challenge to the durability of the fuel injection system components, as it can cause corrosion, further exacerbated by cavitation-induced erosion. In the paper [26], the authors use calculated fluid dynamics (CFD) both to analyze the flow and to predict sites prone to cavitational erosion in e100-powered multi-shaft gasoline injectors (GDi).

The paper [27] presents a study concerning the penetration length, spray angle, and spray pattern were analyzed through spray experiments in which the blend ratio of ethanol–gasoline blended fuel was varied. In addition, a direct injection-type flex fuel vehicle engine test device was built, and the combustion and knocking characteristics were investigated with respect to the ethanol ratio through an engine test. Compared with the brake-specific fuel consumption and the combustion pressure of E0, those of e100 increased by 28.7% (because the lower heating value was lower for e100) and reduced by 11.2%, respectively.

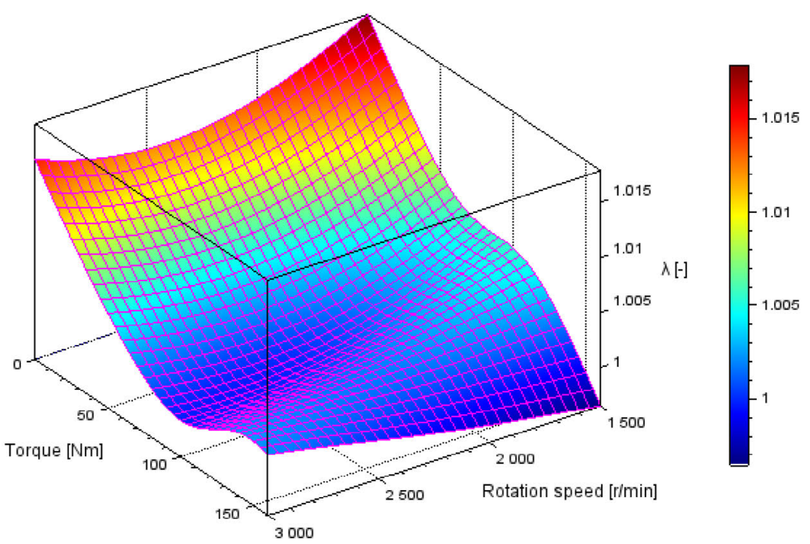

a

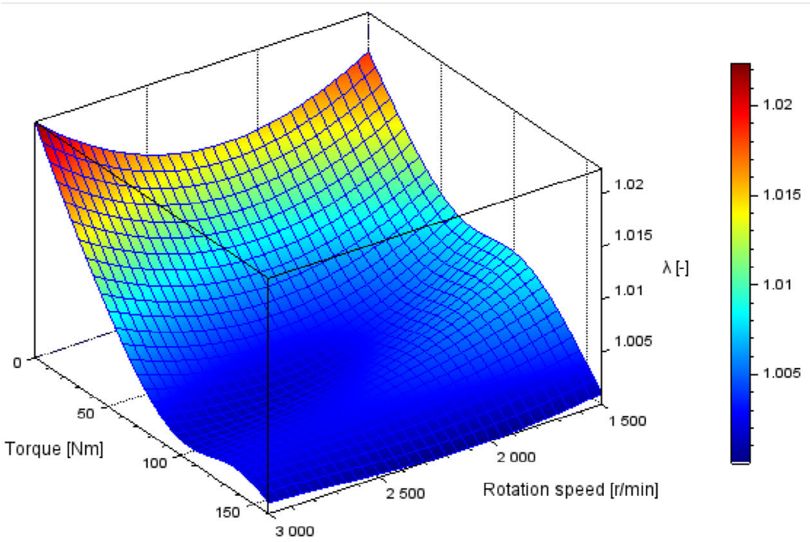

b

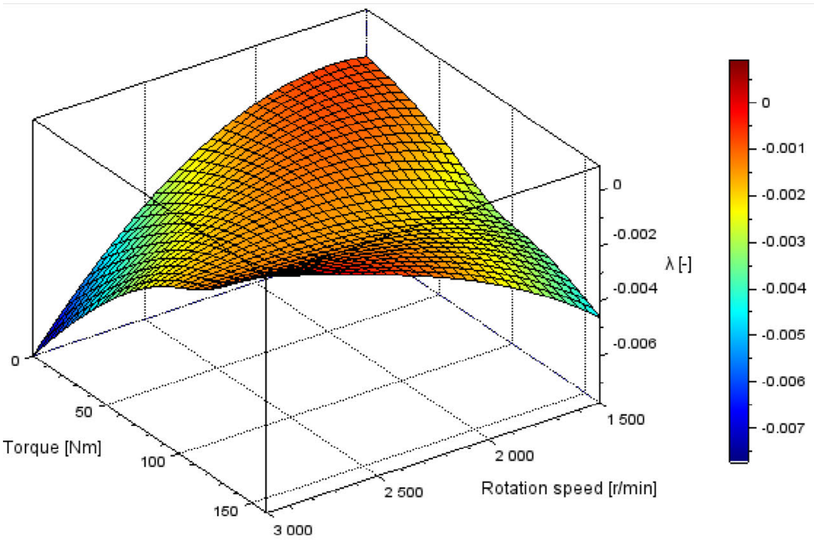

c

Figure 9. Quantitative model of changes in excess air coefficient λ [-] exhaust gas as a function of crankshaft rotational speed [rpm] and engine load ratio [%]: a- fuel 95 octanes, b- fuel 100 octanes, c - differences in the course of the obtained quantitative model of changes in excess air coefficient λ [-] exhaust gas (values for fuel 95 octanes – values for fuel 100 octanes) as a function of crankshaft rotational speed [rpm] engine load ratio [%]

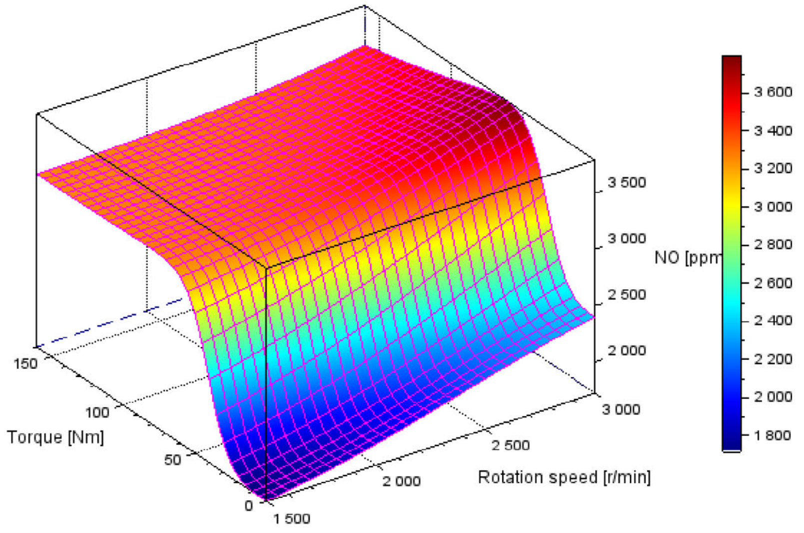

a

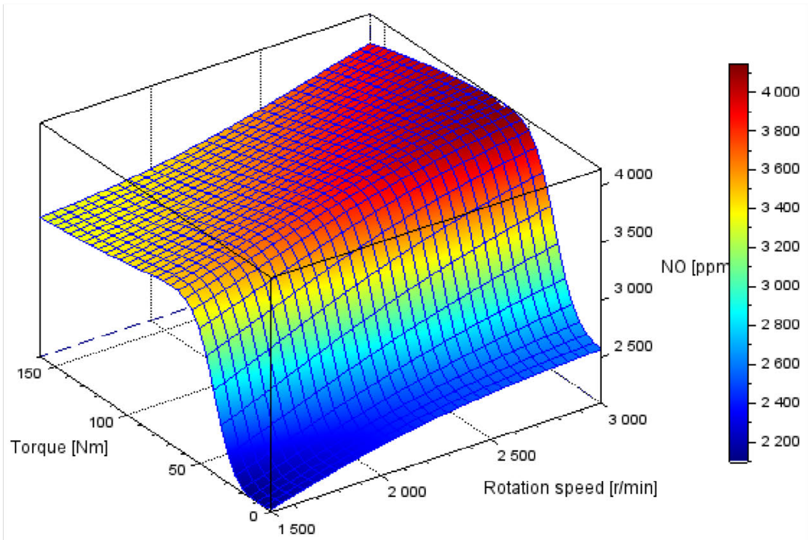

b

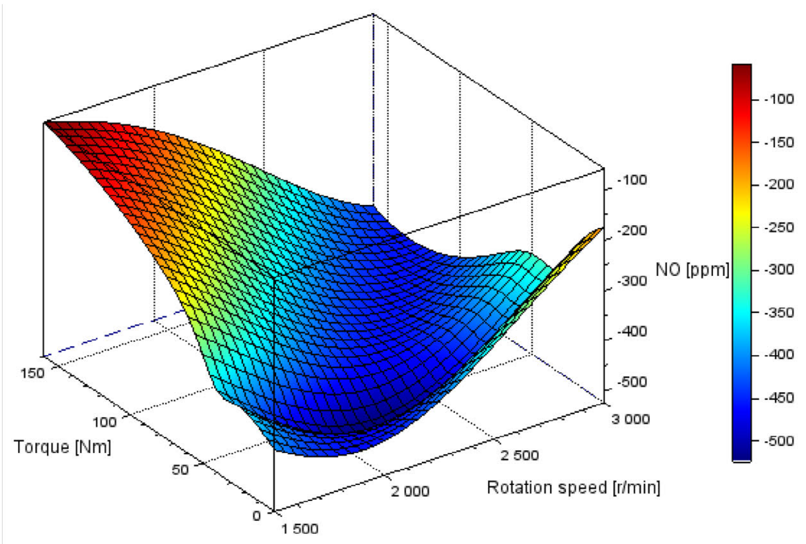

c

Figure 10. Quantitative model of NO oxide changes [ppm] in exhaust gases as a function of crankshaft rotational speed [rpm] and engine load ratio [%]: a- fuel 95 octanes, b- fuel 100 octanes, c - differences in the course of the obtained quantitative model of NO oxide changes [ppm] in exhaust gases (values for fuel 95 octanes – values for fuel 100 octanes) as a function of crankshaft rotational speed [rpm] and the engine load rate [%]

Assessing light flex-fuel vehicle emissions with ethanol/gasoline blends along an urban corridor: A case of Fortaleza/Brazil was the subject of research presented in the publication [28]. In research proposes a comprehensive impact evaluation of an FFV when traveling on BRT corridors, specifically on lanes from mixed traffic, and evaluate the emission factors, specifically on lanes from mixed traffic, composed of a wide variety of vehicle types.

CONCLUSIONS

As a result of comparative tests conducted on 95 and 100 octane fuels on a chassis dynamometer, a number of important conclusions were drawn:

- The engine running on 100 octane fuel demonstrated higher power and torque in the mid-range rpm than on 95 octane fuel. These results suggested that 100 octane fuel promoted better use of the energy contained in the fuel, which translated into better engine performance.
- Based on the test results, the e100 fuel-powered engine was characterized by greater flexibility than the e95 fuel-powered engine due to a significant increase in the maximum torque value.
- With higher engine power for 100 octane fuel, higher emissions of nitrogen oxides (NO and NO_2) were noticed. This was potentially due to the higher combustion temperatures of 100 octane fuel, which favoured the formation of nitrogen oxides.
- The lambda coefficient of CO_2 content and O_2 content are in accordance with the principles of operation of the engine with spark ignition and confirm the correctness of the experiment carried out.
- The contents of other pollutants, such as emissions of carbon dioxide (CO2), hydrocarbons (HC) and carbon oxides (CO), were similar for both fuels.
- The lambda coefficient, measured to assess combustion efficiency, was stable and almost identical for both fuels.

Acknowledgements

This study was financed by the Bialystok University of Technology under the project WZ/WIZ-INZ/4/2022 (Olga Orynycz) and by Institute of Mechanical Engineering, Warsaw University of Life Sciences.

REFERENCES

1. Fuć P, Siedlecki S, Szymlet N, Sokolnicka B, Rymaniak Ł, Dobrzyński M. Exhaust emissions from a Euro 6c compliant pc vehicle in real operating conditions. Journal of KONBiN 2019;49:421-431. 10.2478/jok-2019-0094
2. Krause J, Thiel C, Tsokolis D, Samaras Z, Rota C, Ward A, Prenninger P, Coosemans T, Neugebauer S, Verhoeve, W. EU road vehicle energy consumption and CO2 emissions by 2050 – Expert-based scenarios. Energy Policy 2020; 138: 111224. https://doi.org/10.1016/j.enpol.2019.111224
3. Kim K., Lee J., Kim J. Can liquefied petroleum gas vehicles join the fleet of alternative fuel vehicles? Implications of transportation policy based on market forecast and environmental impact. Energy Policy 2021; 154: 112311. https://doi.org/10.1016/j.enpol.2021.112311
4. Foteinis S, Chatzisymeon E, Litinas A, Tsoutsos T. Used-cooking-oil biodiesel: Life cycle assessment and comparison with first- and third-generation biofuel. Renewable Energy 2020; 153:588-600. https://doi.org/10.1016/j.renene.2020.02.022.
5. Nieuwenhuijsen MJ. Urban and transport planning pathways to carbon neutral, liveable and healthy cities; A review of the current evidence. Environment International 2020;140:105661. https://doi.org/10.1016/j.envint.2020.105661
6. Puricelli S, Cardellini G, Casadei S, Faedo D, Van den Oever AEM, Grosso M. A review on biofuels for light-duty vehicles in Europe. Renewable and Sustainable Energy Reviews 2020;137:110398. https://doi.org/10.1016/j.rser.2020.110398
7. Meng Z, Wang W, Zeng B, Bao Z, Hu Y, Ou J, Liu J. An experimental investigation of particulate emission characteristics of catalytic diesel particulate filters during passive regeneration. Chemical Engineering Journal 2023; 468:143549. https://doi.org/10.1016/j.cej.2023.143549
8. Liu D, Li X, Xie L, Chang J, Kang Y, Zhang Z. Experimental studies on the particulate matter emission characteristics of a lateral swirl combustion system for direct injection diesel engines. Environmental Pollution 2023;330:121756. https://doi.org/10.1016/j.envpol.2023.121756
9. Bielaczyc P, Szczotka A, Woodburn J. An overview of particulate matter emissions from modern light duty vehicles. Combustion Engines. 2013;153(2):101-108. doi:10.19206/CE-117007
10. Bharathiraja B, Jayamuthunagai J, Sudharsanaa T, Bharghavi A, Praveenkumar R, Chakravarthy M, Yuvaraj D. Biobutanol – An impending biofuel for future: A review on upstream and downstream processing tecniques. Renewable and Sustainable Energy Reviews 2017;68:788-807. https://doi.

org/10.1016/j.rser.2016.10.017
11. Zhang M, Ge Y, Wang X, Xu H, Tan J, Hao L. Effects of ethanol and aromatic compositions on regulated and unregulated emissions of E10-fuelled China-6 compliant gasoline direct injection vehicles. Renewable Energy 2021;176:322-333. https://doi.org/10.1016/j.renene.2021.03.029
12. Makkawi Y, Khan M, Pour FH, Moussa O, Mohamed B, Alnoman H, Elsayed Y. A comparative analysis of second-generation biofuels and its potentials for large-scale production in arid and semi-arid regions. Fuel 2023;343:127893. https://doi.org/10.1016/j.fuel.2023.127893
13. Abbasi M, Pishvaee MS, Mohseni S. Third-generation biofuel supply chain: A comprehensive review and future research directions. Journal of Cleaner Production 2021;323:129100. https://doi.org/10.1016/j.jclepro.2021.129100
14. Yang Y, Tian Z, Lan Y, Wang S, Chen H. An overview of biofuel power generation on policies and finance environment, applied biofuels, device and performance. Journal of Traffic and Transportation Engineering (English Edition) 2021;8:534-553. https://doi.org/10.1016/j.jtte.2021.07.002
15. Slavin V, Shuba Y, Caban J, Matijosius J, Rimkus A, Korpach A, Gutarevych S. The Performance of a Car with Various Engine Power Systems – Part I. LOGI – Scientific Journal on Transport and Logistics 2022; 13: 130-140. https://doi.org/10.2478/logi-2022-0012
16. Najjar YSH, Alturki AM. Modeling and simulation of spark ignition engines. Fuel Science and Technology International 1996; 14(8), 993–1018. https://doi.org/10.1080/08843759608947625
17. Sarkan B, Stopka O, Gnap J, Caban J. Investigation of Exhaust Emissions of Vehicles with the Spark Ignition Engine within Emission Control. Procedia Engineering 2017;187:775-782. https://doi.org/10.1016/j.proeng.2017.04.437.
18. Gupta A, Abdel-Gayed R. Qualitative Governing Approach of a Spark Ignition Engine Using Exhaust Gas Recirculation. Energy Procedia 2015;66:97-100. https://doi.org/10.1016/j.egypro.2015.02.052.
19. Adibi-Asl H, Fraser RA, McPhee J. Math-based spark ignition engine modelling including emission prediction for control applications. International Journal of Vehicle Systems Modelling and Testing 2015;10:148-167. https://doi.org/10.1504/IJVSMT.2015.068977.
20. Tucki K, Orynycz OA, Świć A, Wasiak A, Mruk R, Gola A. Analysis of the Possibility of Using Neural Networks to Monitor the Technical Efficiency of Diesel Engines During Operation. Advances in Science and Technology Research Journal. 2023;17(6):1-15. doi:10.12913/22998624/172003.
21. OBD2. Available online: https://www.csselectronics.com/pages/obd2-pid-table-on-board-diagnostics-j1979 (accessed on 19 June 2023)
22. MAHA. Emission measurement technology. Available online: https://www.maha.de/restriction/check-asset/support_documents/dokumente/Brosch%C3%BCren/MAHA/05_Abgasmesstechnik/MET/TD_MAHA_MET_6.3_VP135213_en.pdf (accessed on 19 June 2023)
23. Bocheński C. Fuels and lubricating oils in agriculture. Wydawnictwo SGGW, Warszawa 2005, pp. 10-268.
24. Polcar A, Skrivanek A, Cupera J. The operation of automobile engines on biofuel E85. MECCA Journal of Middle European Construction and Design of Cars 2012; 2; 37-43. DOI: 10.2478/v10138-012-0011-y
25. Schifter I, Diaz L, Rodriguez R, Gómez JP, Gonzalez U.Combustion and emissions behavior for ethanol–gasoline blends in a single cylinder engine. Fuel 2011; 90, 3586-3592. https://doi.org/10.1016/j.fuel.2011.01.034
26. Santos EG, Shi J, Venkatasubramanian R, Hoffmann G, Gavaises M, Bauer W. Modelling and prediction of cavitation erosion in GDi injectors operated with E100 fuel. Fuel 2021; 289,119923. https://doi.org/10.1016/j.fuel.2020.119923
27. Kim Y, Kim WI, Min B, Seo J, Lee K. Experimental investigation of combustion characteristics of ethanol–gasoline blended fuel in a T-GDI engine. Applied Thermal Engineering 2022;208,118168. https://doi.org/10.1016/j.applthermaleng.2022.118168
28. Frutuoso FS, Alves CMAC, Araújo SL, Serra DS, Barros ALBP, Cavalcante FSA, Araújo RS, Policarpo NA, Oliveira MLM. Assessing light flex-fuel vehicle emissions with ethanol/gasoline blends along an urban corridor: A case of Fortaleza/Brazil. International Journal of Transportation Science and Technology 2023; 12, 447-459. https://doi.org/10.1016/j.ijtst.2022.04.001